

Electronic Supplementary Information

**A resettable supramolecular platform for
constructing Scalable Encoders**

Chunrong Yang,^a Shu Yang,^b Lingbo Song,^b Ye Yao,^a Xiao Lin,^a Kaicong Cai,^c Qianfan Yang^{a*} and
Yalin Tang^d

a. College of Chemistry, Sichuan University, Chengdu, 610065, China

b. West China School of Pharmacy, Sichuan University, Chengdu 610064, P. R. China

*c. Fujian Provincial Key Laboratory of Featured Materials in Biochemical Industry, Ningde Normal University,
Ningde, 352100, China.*

d. Institute of Chemistry, Chinese Academy of Sciences, Beijing, 100190, China.

The corresponding author: yangqf@scu.edu.cn

S(a) - Experimental details

Chemicals and materials

DNA oligonucleotides (listed in Tab. S1) were purchased from Sangon Biotechnology Co. Ltd. (Shanghai, China). The cyanine dye *MTC* was synthesized in our lab and the purity was proved by high resolution mass spectrometry (HRMS), high performance liquid chromatography (HPLC), nuclear magnetic resonance (^1H NMR, ^{13}C NMR) and absorption spectroscopy. All the analytical reagent grade chemicals were purchased from Aldrich Ltd. (Shanghai, China) and used as received without further purification. Ultrapure water prepared by ULUPURE (Chengdu, China) ultrapure water system and was used throughout the experiments.

Tab. S1 The DNA oligonucleotides used in this work.

C₀	CCCACCCTCCCACCC	15 nt
C₁	CCACCACCACCACAACCACCACCACCAAA	29 nt
C₂	CCAACCACACCAACC	15 nt
C₃	CCACCACCACCA	12 nt
C₄	CCCTAACCCCTAACCCCTAACCCCTAA	24 nt
C₅	AACCCACCC	9 nt
C₆	TTTTCCACACCTTTT	15 nt
G₀	GGAGGAGGAGGA	12 nt
G₁	TGAGGGTGGGGAGGGTGGGGAA	22 nt
G₂	GTGGGTAGGGCGGGTTGGTGTGGTTGG	27 nt
G₃	GGTGGTGGTGGTGTGGTGGTGGTGGTTT	29 nt
G₄	TTAGGGTTAGGGTTAGGGTTAGGG	24 nt
G₅	GGGTGGGTGGGTGGG	15 nt
G₆	GGTGGTGGTGGT	12 nt

Instruments and equipment

The absorption spectra were acquired using a 10 mm quartz cuvette on an EVOLUTION 201 spectrophotometer (Thermo SCIENTIFIC, USA) at 37 °C in a 10 mm quartz cell, and the scan range is 400-750 nm. The melting curves of *MTC* aggregates were collected by heating the samples to 80 °C at a rate of 0.01 °C / s.

The fluorescence spectra were collected with a F-4600 spectrophotometer (HITACHI, Japan) in a 10 mm quartz cell, Xenon arc lamp was used as the excitation light source. Both the excitation and emission slits were 5 nm, the PMT voltage was 400 V. The excitation wavelength was 530 nm and emission wavelength were 530 -750 nm. The fluorescence intensity variation curve was collected by heating the samples to 75 °C at a rate of 0.01 °C / s.

The circular dichroism spectra were collected with a Chirascan Plus spectrophotometer (AppliedPhotophysics, UK) in a 10 mm quartz cell. The bandwidth is 1 nm. High purity N₂ was used as a shielding gas before and during the collection and all data were collected at room temperature.

Sample preparation

The DNase I was dissolved in 10 mM, pH 6.5 Tris-Ac buffer solution to 5 mg/mL. The 200 μM *MTC* stock solution was prepared by dissolving 7.67 mg *MTC* powder in 50 mL methanol and stored in darkness. The concentration of *MTC* stock solution is corrected by diluting 50 μL stock solution to 1000 μL with methanol, measuring its absorbance at 573 nm and calculating the actual concentration via Lambert-beer's law. The DNA stock solutions were prepared by dissolving certain amounts of oligonucleotides in 10 mM, pH 6.5 Tris-Ac buffer solution. The concentrations of DNA were determined by measuring absorbance at 260 nm. All these metal salts were dissolved by ultrapure water. The stock solution of AgNO₃, MgCl₂, Cu(NO₃)₂, Pb(NO₃)₂, MnCl₂, CoSO₄, ZnSO₄, NiSO₄, Ca(NO₃)₂ was 10 mM and the stock solution of MnCl₂ is 50 mM.

Operations of the EC circuits

To demonstrate the logic functions of the platform better, the input conditions were optimized in each circuit. All the stimuli, metal ions and DNA strands, were incubated with *MTC* in dark at 37 °C for 30 min before the measurement.

In the 4-to-2 and 7-to-3 ECs, 30 μL *MTC* stock solution (200 μM) and metal ions were added into 10 mM, pH 6.5 Tris-Ac buffer solution. The total volume of the reaction sample is 1000 μL . The final concentration of the ions is 0.4 mM Ag^+ , 0.4 mM Mg^{2+} , 0.4 mM Pb^{2+} , 2 mM Mn^{2+} , 0.08 mM Co^{2+} , 0.2 mM Zn^{2+} and 0.4 mM Ca^{2+} . When all the stock solution added in, the samples were stand at room temperature for 5 min to fully mixed and then incubated at 37 °C in dark for 30 min.

In the 8-to-3 and 14-to-4 ECs, 30 μL *MTC* stock solution (200 μM), DNA and metal ions were added into 10 mM, pH 6.5 Tris-Ac buffer solution. The total volume of the reaction sample is 1000 μL . The final concentration of the ions is same as that in 7-to-3 EC. The final concentration of the DNA strands is 0.5 μM C_0 , 0.5 μM C_1 , 0.5 μM C_2 , 0.5 μM C_3 , 0.5 μM C_4 , 0.5 μM C_5 , 0.5 μM C_6 , 1.5 μM G_0 , 0.3 μM G_1 , 0.5 μM G_2 , 0.3 μM G_3 , 5 μM G_4 , 0.7 μM G_5 and 0.5 μM G_6 . When all the stock solution added in, the samples were stand at room temperature for 5 min to fully mixed and then incubated at 37 °C in dark for 30 min.

Resetting of the EC circuits

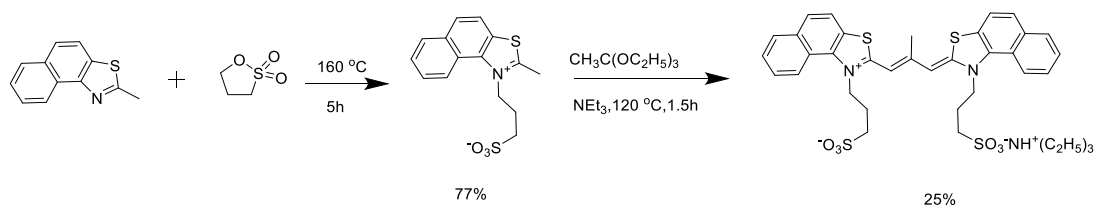
For the resetting of the 4-to-2 and 7-to-3 ECs, EDTA was added the samples that have been implemented encoder's operation. The concentration of EDTA in each sample was in line with the corresponding metal ion, i.e., 0.08 or 0.4 or 3 mM. After incubated at 40 °C in dark for 20 min, absorption spectra were collected.

For the resetting of the 8-to-3 and 14-to-4 ECs, we added EDTA and DNase I separately. To avoid the heavy metal ions disturbing the hydrolysis process, EDTA was added into the system to complex the ions in advance. After incubated at 37 °C for 10 min, 5 μL DNase I (5mg/mL) was added, and the samples were further incubated at 25°C for 30 min. Finally, the samples were heated at 70 °C for 10 min to

inactivate the enzyme. Since the metal ions were chelated by EDTA in advance, subsequent enzymatic cleavage reactions would not be affected by the ions.

S(b) - Synthesis and identification of *MTC*

1. Synthesis of *MTC*



The cyanine dye *MTC* was synthesized according to the methods of Hamer¹ and Ficken². In the first step, 0.51 g (2.56 mmol) 2-methylnaphthyl-thiazole and 1.05 g (8.59 mmol) 1,3-propyl sulfonate were mixed and reaction at 160 °C for 5 h. The reaction was traced with TLC. The mixture was then recrystallized in diethyl ether. After evaporated to dryness in vacuum 0.63 mg (77% yield) solid was obtained. Then 0.52 g solid (1.617 mmol), 0.53 g (3.267 mmol) triethyl orthoacetate, 1.05 g phenol (11.16 mmol) and 0.5 mL triethylamine were mixed and then heated at 120 °C for 1.5 h. When the reaction completed, ether was used to deal with the product and then methanol was used to recrystallization. After evaporated to dryness in vacuum 0.30 mg (25% yield) solid was obtained.

2. HRMS-ESI

*HRMS(ESI) m/z $[M-H]^- = 665.09069$

The calculated exact mass of $C_{32}H_{29}N_2O_6S_4^-$ is 665.09139.

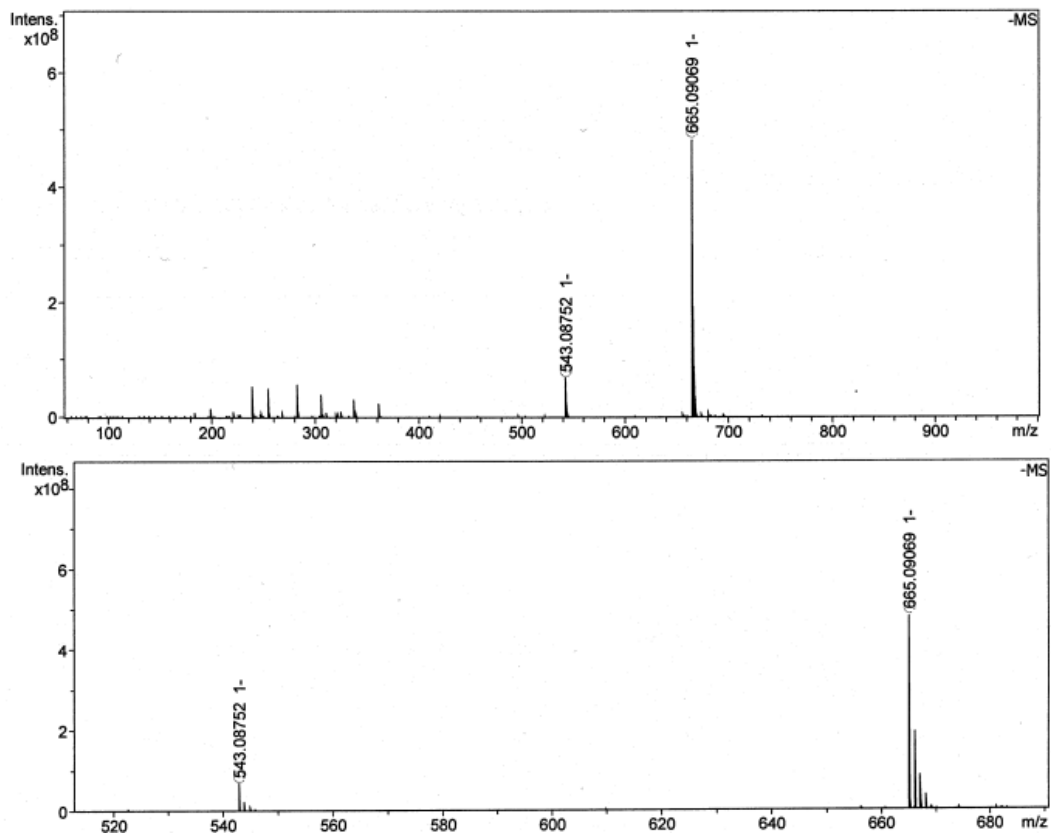


Fig. S1 The HRMS(ESI) spectrum of cyanine dye *MTC*.

3. $^1\text{H-NMR}$ spectrum

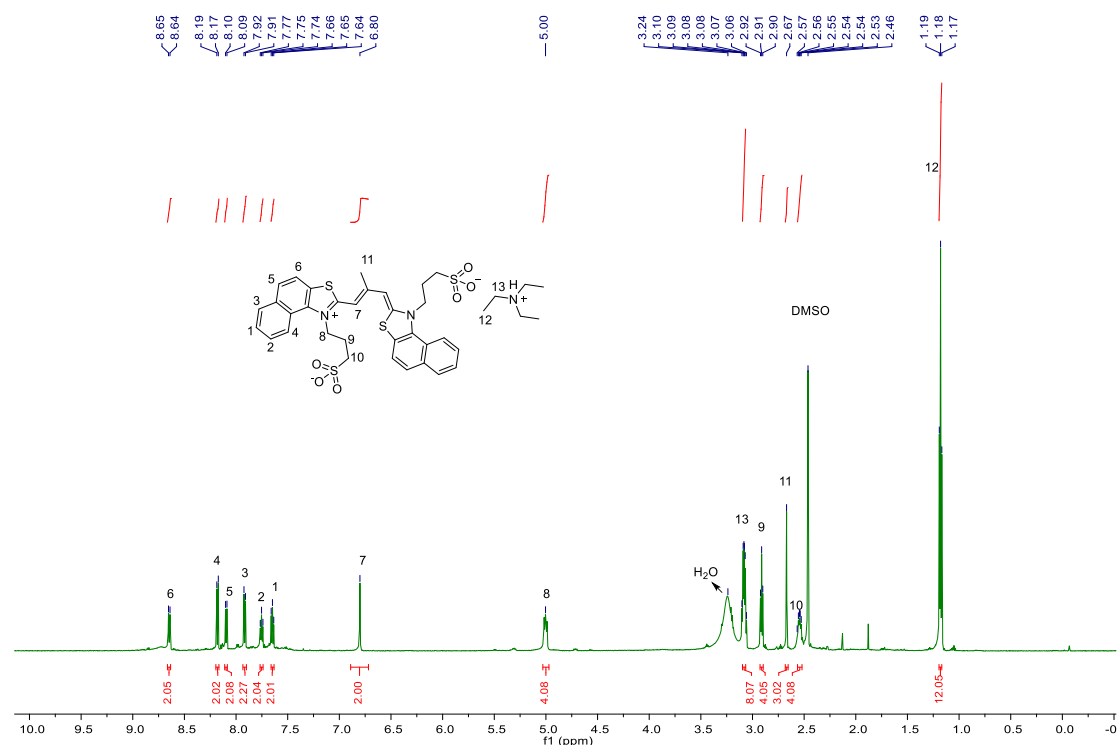


Fig. S2 The $^1\text{H-NMR}$ spectrum of cyanine dye *MTC* in $\text{DMSO-}d_6$.

$^1\text{H NMR}$ (600 MHz, $\text{DMSO-}d_6$) δ 8.65 (d, $J = 8.7$ Hz, 2H), 8.18 (d, $J = 8.6$ Hz, 2H), 8.09 (d, $J = 8.2$ Hz, 2H), 7.92 (d, $J = 8.6$ Hz, 2H), 7.75 (t, $J = 7.7$ Hz, 2H), 7.66 - 7.63 (m, 2H), 6.80 (s, 2H), 5.06 - 4.97 (m, 4H), 3.10 - 3.05 (m, 8H), 2.91 (t, $J = 6.6$ Hz, 4H), 2.67 (s, 3H), 2.56 - 2.52 (m, 4H), 1.19 (d, $J = 7.2$ Hz, 12H).

According to the $^1\text{H-NMR}$ spectrum, the signals are in line with *MTC*'s structure but the integrations at 1.18 and 3.10 ppm show there are excessive triethylamine in the sample.

The signals at 1.18 and 3.10 ppm are assigned to the ethyl groups on the triethylammonium ion and the integration ratio (12:8) is in accordance with the triethylamine structure (3:2). Theoretically, the integrations at should be 9H (1.18 ppm) and 6H (3.10 ppm), respectively. However, in the synthesis process, the excessive triethylamine is difficult to eliminate completely. The excess signals may come from the residual triethylamine in the synthesis. Since small amount of triethylamine would not influence the feature of *MTC*, the sample was used without further purification.

4. ^{13}C -NMR spectrum

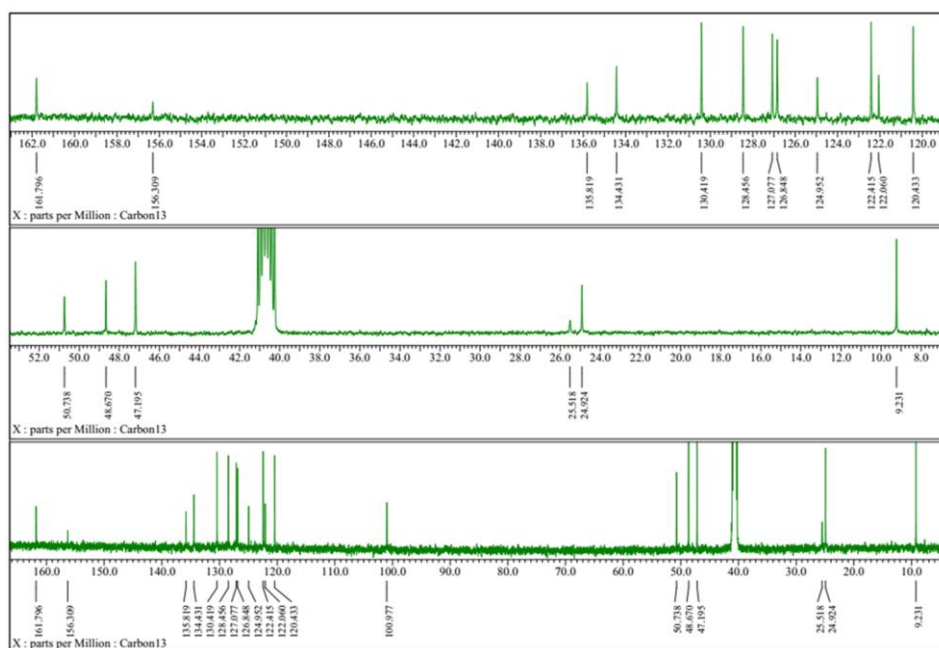


Fig. S3 The ^{13}C -NMR spectrum of cyanine dye *MTC* in DMSO-d_6 .

^{13}C NMR (151 MHz, DMSO-D_6) δ 161.80, 156.31, 135.82, 134.43, 130.42, 128.46, 127.08, 126.85, 124.95, 122.41, 122.06, 120.43, 100.98, 50.74, 48.67, 47.20, 25.52, 24.92, 9.23

5. HSQC and HMBC spectra

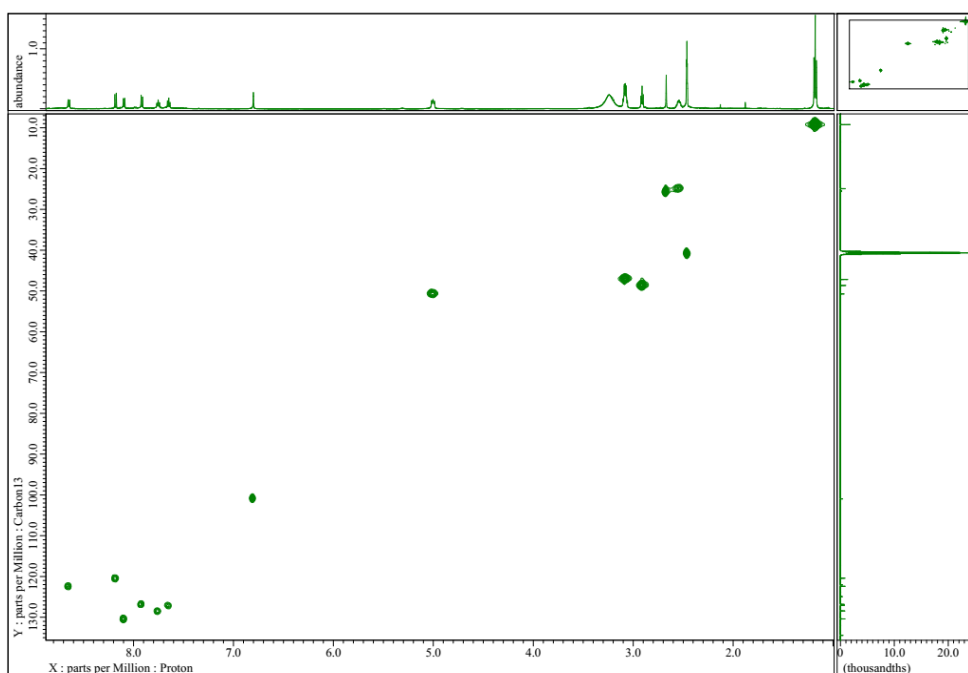


Fig. S4 The HSQC spectrum of cyanine dye *MTC* in DMSO-d_6 .

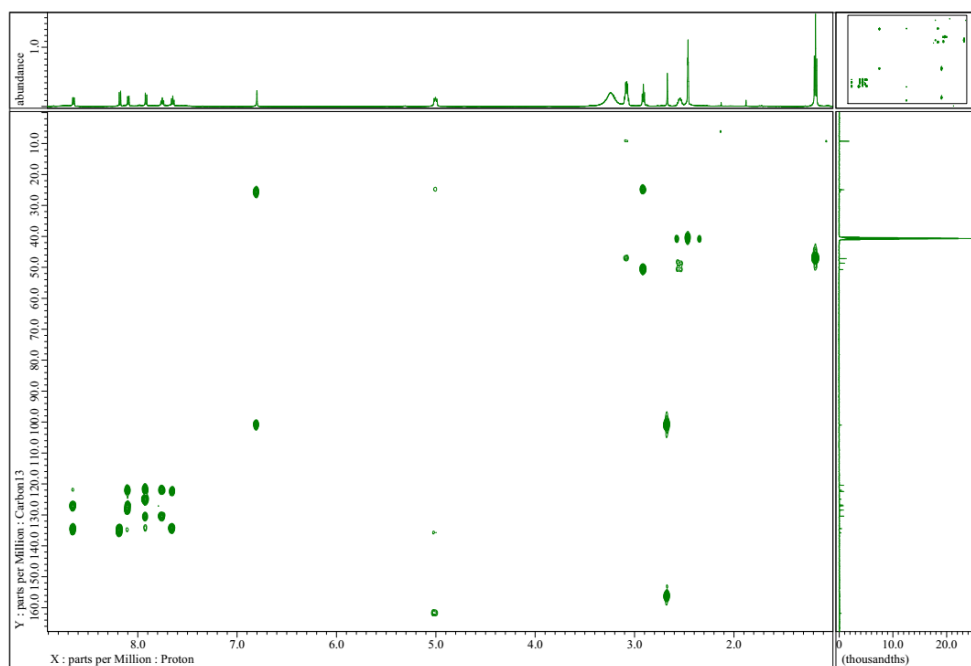
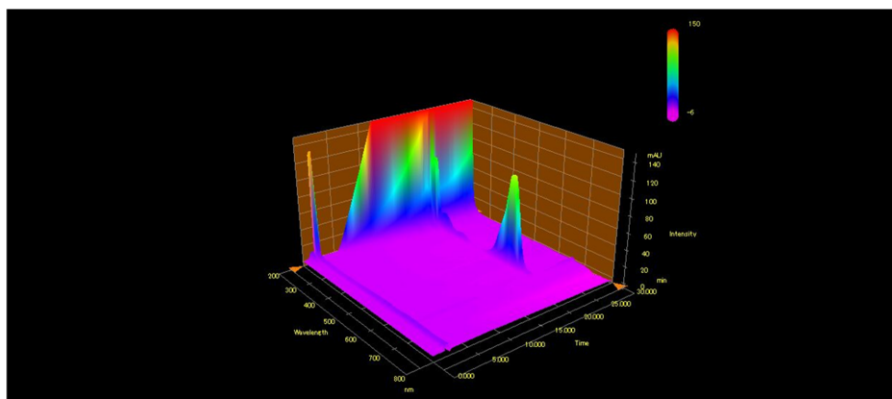


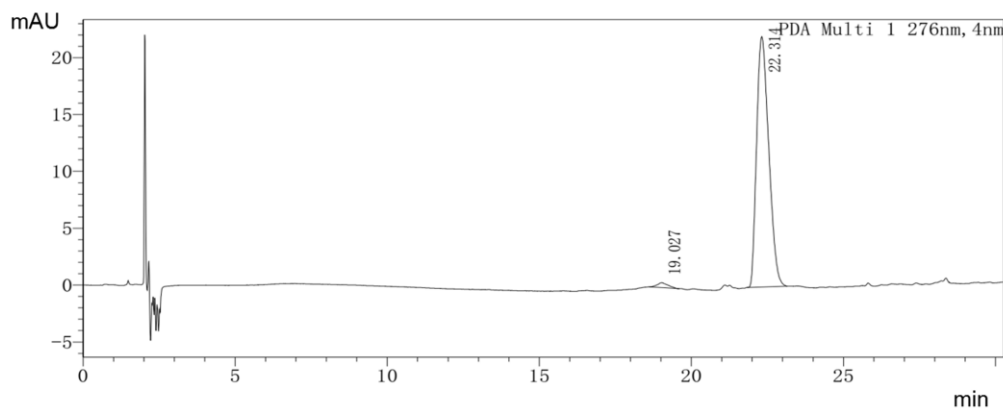
Fig. S5 The HMBC spectrum of cyanine dye *MTC* in DMSO-d₆.

5. HPLC

A

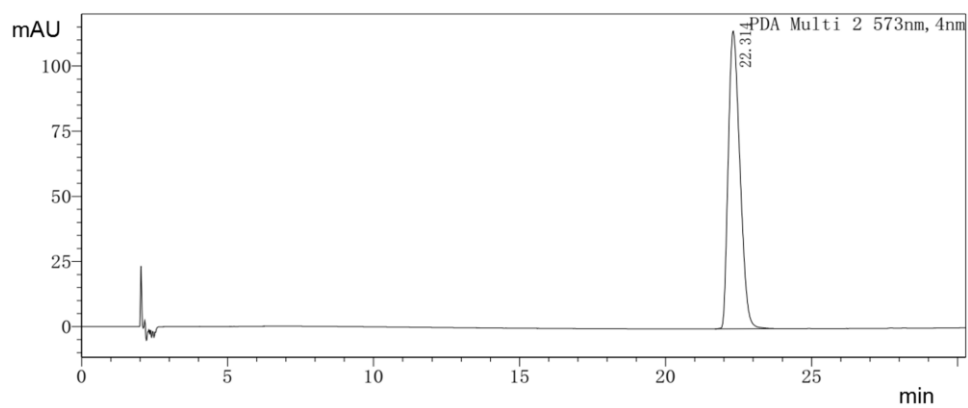


B



Peak No.	Retention Time	Area	Area%	Height
1	19.027	10730	1.728	435
2	22.314	610315	98.272	22017

C



Peak No.	Retention Time	Area	Area%	Height
1	22.314	3174113	100	114222

Fig. S6 The HPLC trace of cyanine dye *MTC* in CH₃OH-H₂O solution (5-100% CH₃OH). Inertsil C₁₈ Column, flow rate 1.0 mL/min, T = 30 °C. (A)DAD:200-800 nm. (B) λ = 276 nm. (C) λ = 573 nm.

6. UV/Vis spectrum research and absorption coefficient calculation

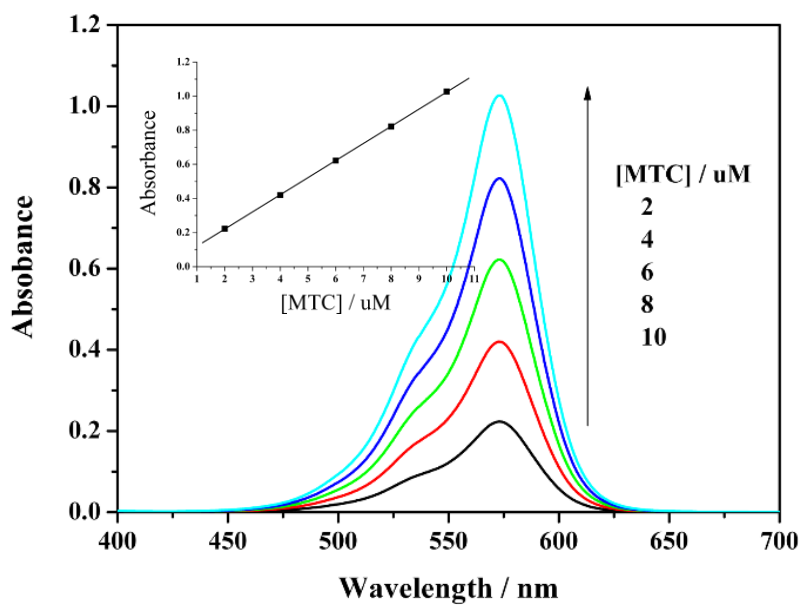


Fig. S7 The absorption spectra of *MTC* monomer in methanol. Insert gives the curve of the absorbance at 573 nm against the concentration of *MTC* monomer.

Based on Lambert-beer's law, the molar absorption coefficient of *MTC* monomer is

$$\varepsilon_{1cm,573nm}^M = 1.00 \times 10^6 M^{-1} \cdot cm^{-1}.$$

S(c) - The study on *MTC* assembly behavior

1. The regulation via metal ions

According to the regulation, we optimized the concentration of each ions to 0.4 mM Ag^+ , 0.4 mM Mg^{2+} , 0.4 mM Cu^{2+} , 0.4 mM Pb^{2+} , 2 mM Mn^{2+} , 0.08 mM Co^{2+} , 0.2 mM Zn^{2+} , 0.2 mM Ni^{2+} and 0.4 mM Ca^{2+} in encoder construction. And we further plotted the normalized absorbance of each assembly states as bar charts in Fig. S9.

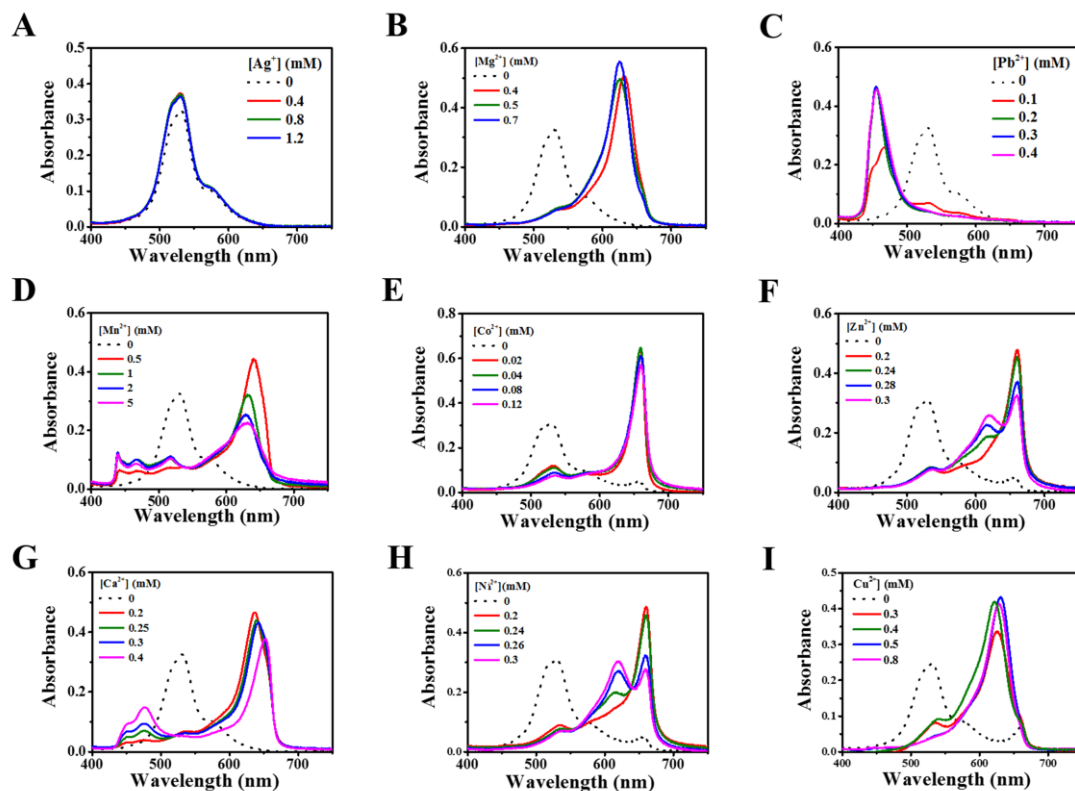


Fig. S8 The regulation of metal ions on 6 μM *MTC* in 10 mM, pH 6.5 tris-Ac buffer solution.

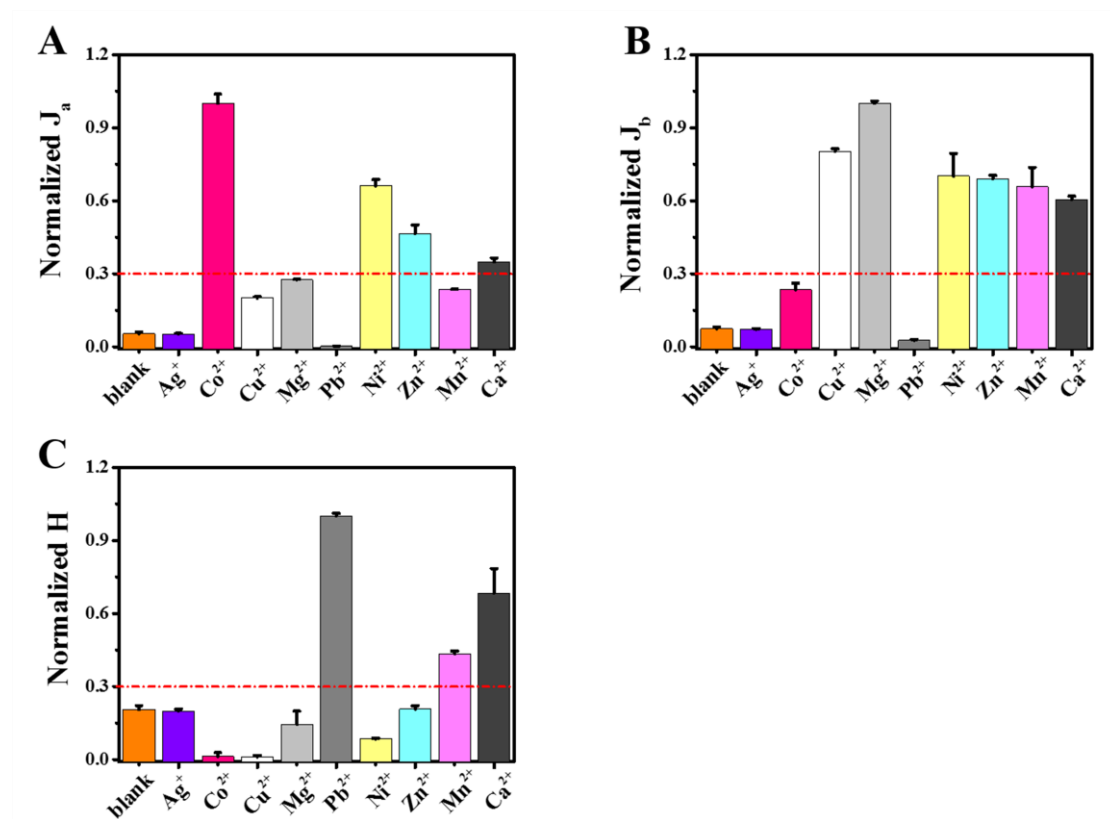


Fig. S9 The normalized 6 μ M *MTC* J_a , J_b and H signals induced by nine ions, i.e., 0.4 mM Ag^+ , 0.08 mM Co^{2+} , 0.4 mM Cu^{2+} , 0.4 mM Mg^{2+} , 0.4 mM Pb^{2+} , 0.2 mM Ni^{2+} , 0.2 mM Zn^{2+} , 2 mM Mn^{2+} and 0.4 mM Ca^{2+} 10 mM, pH 6.5 tris-Ac buffer solution. The normalized absorbance value higher 0.3 defined as “1”, otherwise as “0”.

2. The reverse regulation via EDTA

For the resetting process, we used EDTA to chelate various metal ions. The conditional stability constants ($\lg K'$) of the seven ions at pH 7.0 are: 3.9 (Ag^+), 5.3 (Mg^{2+}), 14.5 (Pb^{2+}), 10.6 (Mn^{2+}), 12.9 (Co^{2+}), 13.1 (Zn^{2+}), 7.3 (Ca^{2+}), indicating that all of these ions can be well eliminated by EDTA.

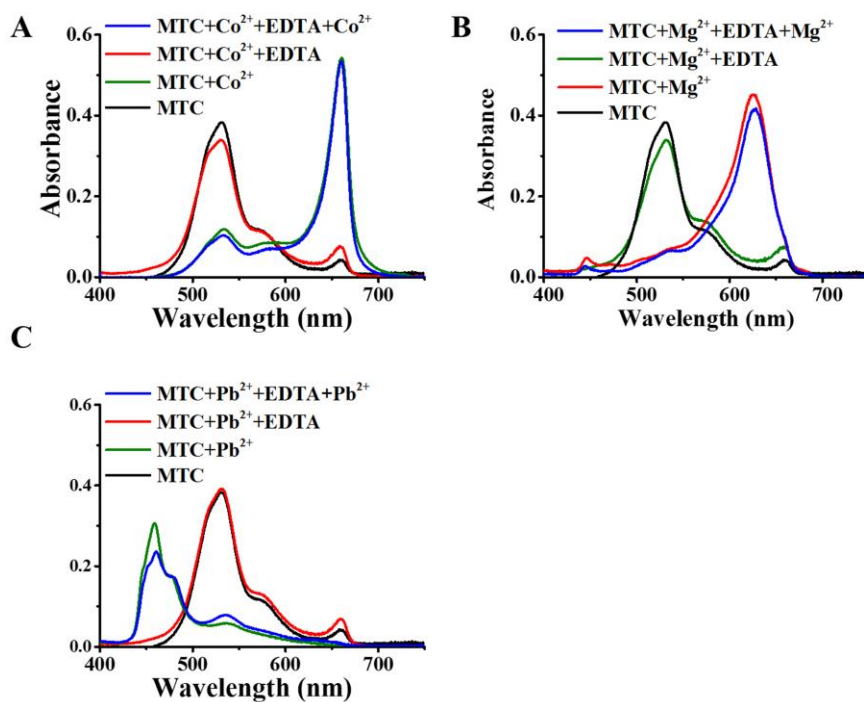


Fig. S10 The inputting-resetting performance of 6 μM *MTC* in 10 mM, pH 6.5 tris-Ac buffer solution. (A) 0.08 mM Co^{2+} and 0.08 mM EDTA. (B) 0.4 mM Mg^{2+} and 0.4 mM EDTA. (C) 0.4 mM Pb^{2+} and 0.4 mM EDTA.

3. The interaction with DNA

The influence of metal ions on the DNA structures have been studied by circular dichroism (CD) spectroscopy. As shown in Fig. S11, under the effects of different metal ions, the seven guanine-rich (G-rich) DNA strands (G_0 - G_6) can fold into several secondary structures: 1) random coil single strands (termed SS-G) that have no obvious characteristic CD signal; 2) parallel G-quadruplex with a positive signal around 262 nm and a negative signal around 240 nm³; 3) antiparallel G-quadruplex induced by Pb^{2+} with a positive signal around 315 nm⁴; 4) Ag^+ induced feature positive signal around 285 nm and 230 nm⁵. The results were summarized in Tab. S2 and the highlighted parts are the combination mode of DNA and metal ion used in this work.

In our design strategy, the DNA strands were introduced as parts of inputs to produce additional output signal (M-FI). We therefore studied the fluorescence intensity changes as a function of DNA concentration in different metal ion/DNA combination modes. As shown in Fig. S10, the fluorescence intensity of *MTC* induced by G-rich DNA strands are 5-160 folds of that induced by C-rich strands (take C_1 as the example) inferring the stronger interaction between *MTC* and the G-rich strands. Due to the complicated secondary structures (ss-G, parallel and antiparallel G-quadruplex) and various binding ratios, it is hard to calculate the accurate association constants of *MTC* and the DNA strands. Instead, we use the linear fit slopes to roughly evaluate the binding abilities of the DNA strands to *MTC*. As shown in Fig. S10, the slopes of G-DNA strands are at least 10 times than that of C_1 , indicating that although the G-rich DNA strands can present various secondary structures, the logic function can be implemented properly.

It is reported that parallel G-quadruplex presents much stronger interaction with *MTC*⁶. Therefore, we calculated the binding constant of G_1 G-quadruplex induced by Mg^{2+} and *MTC*. As shown in Fig. S13, according to the tangent fitting result, a 1:1 binding model for *MTC* with G_1 was confirmed by the Job's plot analysis⁷ and the binding constant was $1.083 \times 10^5 \text{ M}^{-1}$ in the presence of 0.4 mM Mg^{2+} .

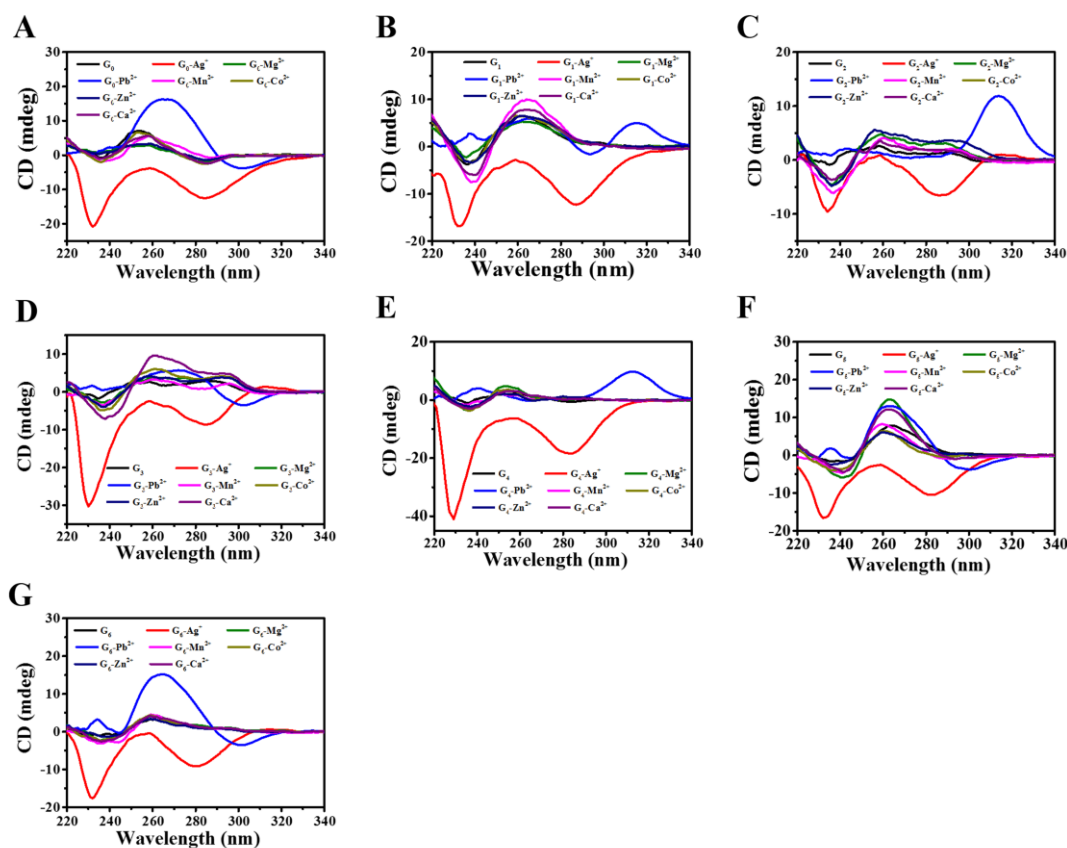


Fig. S11 Circular dichroism spectra of G_0 - G_6 under different metal ions conditions: none metal ions, 0.4 mM Ag^+ , 0.4 mM Mg^{2+} , 0.4 mM Pb^{2+} , 2 mM Mn^{2+} , 0.08 mM Co^{2+} , 0.2 mM Zn^{2+} , 0.4 mM Ca^{2+} . The concentration of DNA is 5 μ M.

Tab. S2 The influence of metal ions on the DNA strands G_0 - G_6 .

	G_0	G_1	G_2	G_3	G_4	G_5	G_6
none metal ions	SS-G	parallel G-quadruplex	SS-G	SS-G	SS-G	parallel G-quadruplex	SS-G
Ag^+	Ag-DNA	Ag-DNA	Ag-DNA	Ag-DNA	Ag-DNA	Ag-DNA	Ag-DNA
Mg^{2+}	SS-G	parallel G-quadruplex	SS-G	SS-G	SS-G	parallel G-quadruplex	SS-G
Pb^{2+}	parallel G-quadruplex	antiparallel G-quadruplex	antiparallel G-quadruplex	SS-G	antiparallel G-quadruplex	parallel G-quadruplex	parallel G-quadruplex
Mn^{2+}	SS-G	parallel G-quadruplex	SS-G	SS-G	SS-G	parallel G-quadruplex	SS-G
Co^{2+}	SS-G	parallel G-quadruplex	SS-G	SS-G	SS-G	parallel G-quadruplex	SS-G
Zn^{2+}	SS-G	parallel G-quadruplex	SS-G	SS-G	SS-G	parallel G-quadruplex	SS-G
Ca^{2+}	SS-G	parallel G-quadruplex	SS-G	SS-G	SS-G	parallel G-quadruplex	parallel G-quadruplex

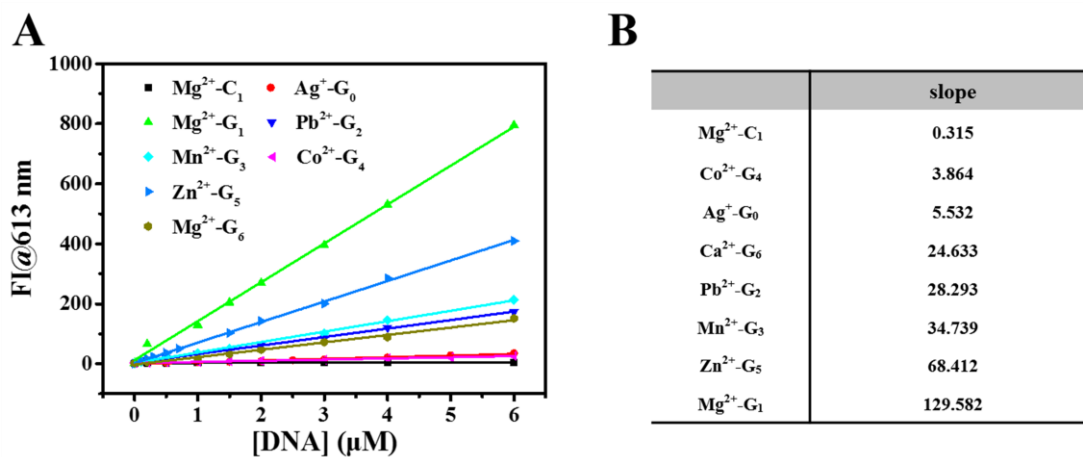


Fig. S12 (A) The titration curves of 6 μM *MTC* monomer fluorescence intensity against the concentration of DNA. (B) The linear fit slopes of each DNA strands.

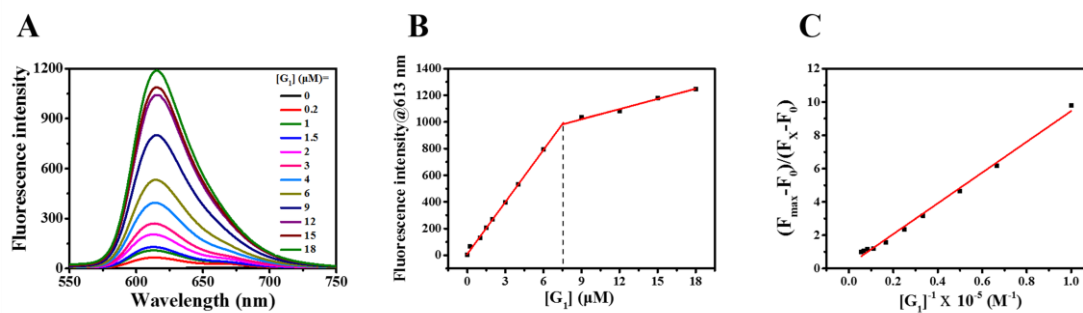


Fig. S13 The fluorescence titration of G_1 in 10 mM, pH 6.5 tris-Ac buffer solution with 0.4 mM Mg^{2+} and 6 μM *MTC*. (A) The fluorescence spectra, (B) the linear fitting curve and (C) the $(F_{\text{max}} - F_x) / (F_x - F_0)$ as a function of $[G_1]^{-1} \times 10^5 \text{ M}^{-1}$.

4. Kinetic study on *MTC* assembly/disassembly

As shown in Fig. S14A-C, the assembly process of H-, J_b- and J_a-aggregates, regulated by Pb²⁺, Mg²⁺ and Co²⁺ respectively, can reach balance within 30 min and *MTC* can produce dramatic fluorescence signal with DNA in 2 min. Fig. S14D-F show that the simultaneous assembly of several aggregates regulated by Mn²⁺, Zn²⁺ and Ca²⁺ are dynamic, and *MTC* prefers to firstly assemble to unstable J-aggregates and then converses to more stable H-aggregates with time. Considering the logical feature of encoder, we optimized the operation time of the ECs to 30 min.

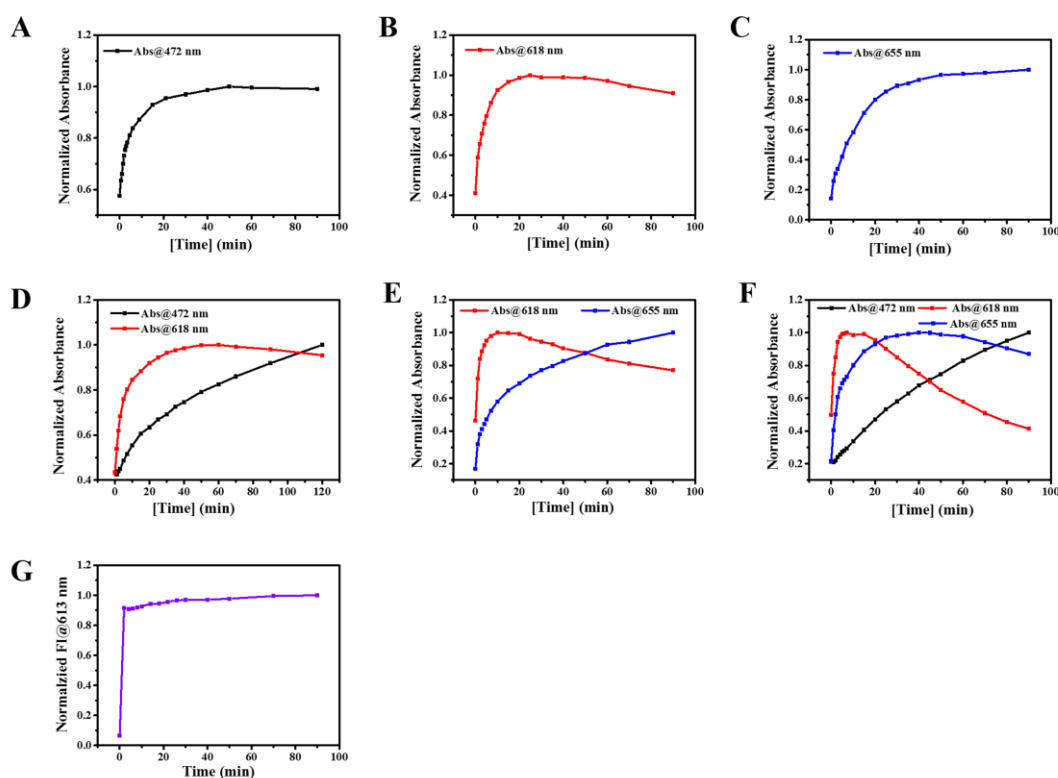


Fig. S14 Kinetics of the *MTC* aggregation and DNA binding processes. Time traces for the H-aggregates stabilized by 0.4 mM Pb²⁺ (A), J_b-aggregates stabilized by 0.4 mM Mg²⁺ (B), J_a-aggregates stabilized by 0.08 mM Co²⁺(C), mixture of H- and J_b-aggregates stabilized by 2 mM Mn²⁺(D), mixture of J_a- and J_b-aggregates stabilized by 0.2 mM Zn²⁺ (E), mixture of H-, J_a- and J_b-aggregates stabilized by 0.4 mM Ca²⁺ (F), and fluorescence (FI@613 nm) induced by the mixture of 0.3 μM G₁ and 0.4 mM Mg²⁺(G). The concentration of *MTC* is 6 μM.

The kinetics of the resetting processes were also studied. As shown in Fig. S15, the H-, J_b- and J_a-aggregates induced by Pb²⁺, Mg²⁺ and Co²⁺ respectively can be

disassembled by EDTA within 10 min, and the enzymatic process can be finished within 30 min.

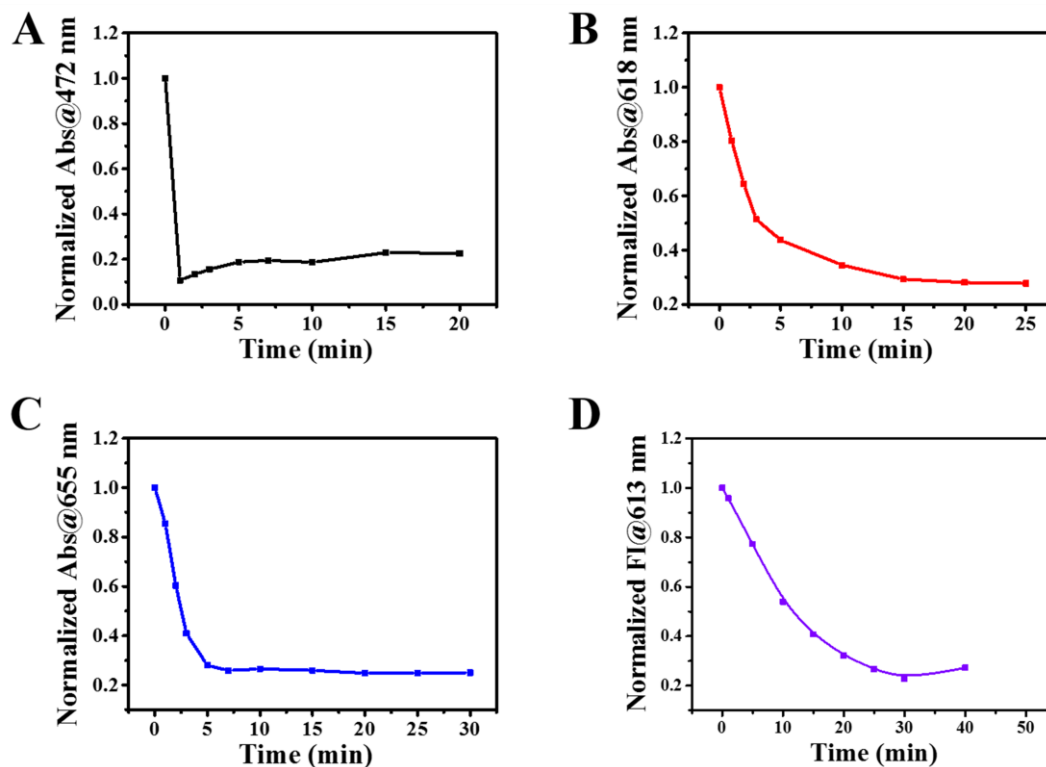


Fig. S15 Kinetics of the resetting processes. (A) The H-aggregates is disassembled by 0.4 mM EDTA. (B) The J_b -aggregates is disassembled by 0.4 mM EDTA. (C) The J_a -aggregates is disassembled by 0.08 mM EDTA. (D) The G_1 DNA hydrolyzed by 5 μ L DNase I (5 mg/mL). The H-aggregates is stabilized by 0.4 mM Pb^{2+} , J_b -aggregates stabilized by 0.4 mM Mg^{2+} , J_b -aggregates stabilized by 0.08 mM Co^{2+} . In digestion, 0.3 μ M G_1 is mixed with 0.4 mM Mg^{2+} . The concentration of *MTC* in all situations is 6 μ M.

5. Thermodynamic study on *MTC* assembly/disassembly

As shown in Fig. S16, the thermodynamic stabilities of H-, J_a -, J_b -aggregates are as follow: H- aggregates > J_a - aggregates > J_b -aggregates, and all the aggregates can be disassembled with the increase of temperature. In addition, we also monitored the fluorescence intensity variation as a function of temperature. Fig. S16-G shows that the fluorescence intensity at 613 nm decreases significantly when temperature increased, and the intensity drops to half at 51.5 °C.

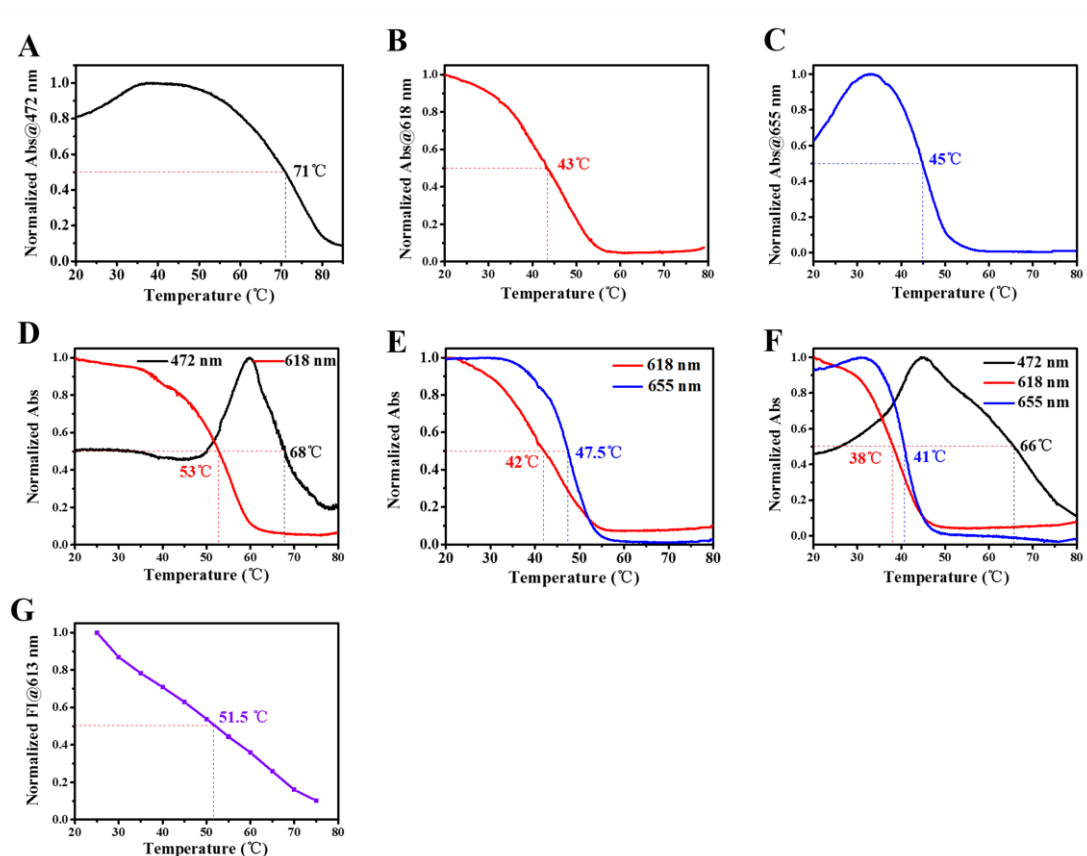


Fig. S16 The melting curves of 6 μM *MTC* at different input conditions: (A) The H-aggregates stabilized by 0.4 mM Pb^{2+} . (B) The J_b -aggregates stabilized by 0.4 mM Mg^{2+} . (C) The J_a -aggregates stabilized by 0.08 mM Co^{2+} . (D) The H- and J_b -aggregates stabilized by 2 mM Mn^{2+} . (E) The J_a - and J_b -aggregates stabilized by 0.2 mM Zn^{2+} . (F) The H-, J_a - and J_b -aggregates stabilized by 0.4 mM Ca^{2+} . (H) The fluorescence induced by the mixture of 0.3 μM G_1 and 0.4 mM Mg^{2+} . The heating rate is 0.01 °C/s.

S(d) - The construction of the ECs

1. The original spectra of the 4-to-2 and 7-to-3 ECs

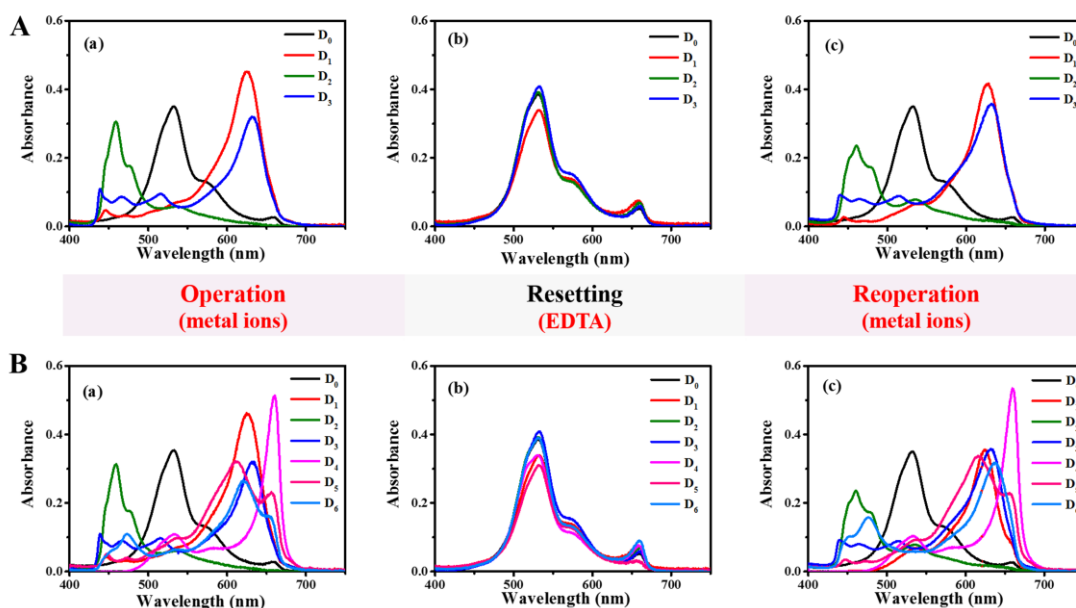


Fig. S17 (A) The absorption spectra of 4-to-2 EC: operation (a), resetting (b) and reoperation (c). (B) The absorption spectra of 7-to-3 EC: operation (a), resetting (b) and reoperation (c). The concentration of *MTC* is 6 μM .

2. The design of the 4-to-2 EC using J_a and J_b as outputs

Based on the *MTC* platform, another 4-to-2 EC was also performed, using J_a and J_b as outputs, and 0.4 mM Ag^+ , 0.4 mM Cu^{2+} , 0.08 mM Co^{2+} and 0.2 mM Ni^{2+} as inputs. In the initial state, *MTC* is in the form of dimer in 10 mM, pH 6.5 tris-Ac buffer solution. The Ag^+ in D_0 channel has no influence on *MTC* dimer, therefore the readout (J_b , J_a) is (0, 0). In D_1 channel, Cu^{2+} induces the formation of J_b -aggregates, resulting in (1, 0), while Co^{2+} induces the formation of J_a -aggregates, resulting in (0, 1) in D_2 channel. In D_3 channel, *MTC* is induced to a mixture of J_a - and J_b -aggregates by Ni^{2+} , resulting in (1, 1).

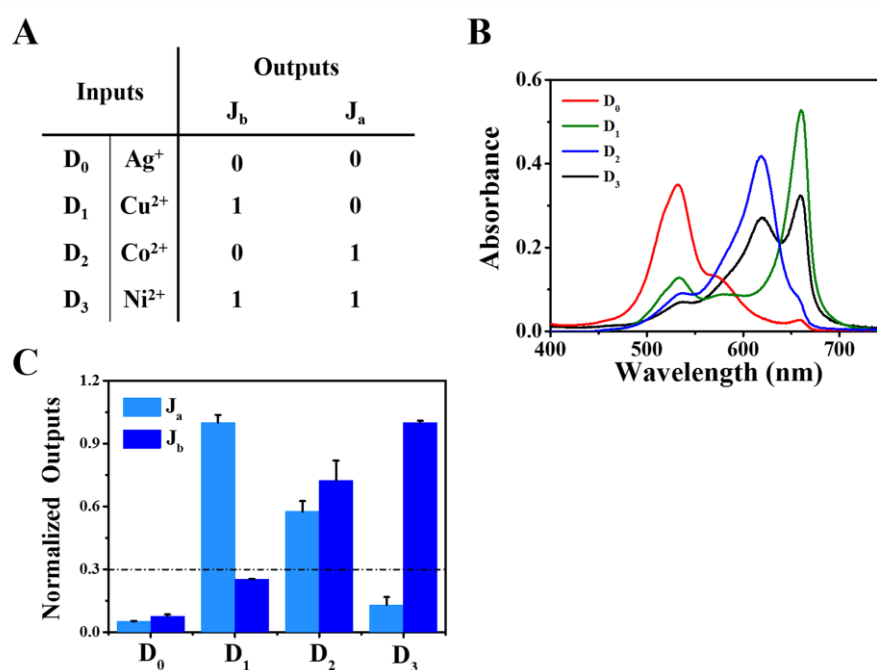


Fig. S18 The design of the 4-to-2 EC using J_a and J_b as outputs. (A) The schematic truth table. (B) The absorption spectra. (C) The normalized outputs. The concentration of *MTC* is 6 μ M.

3. The spectra of the 8-to-3 EC

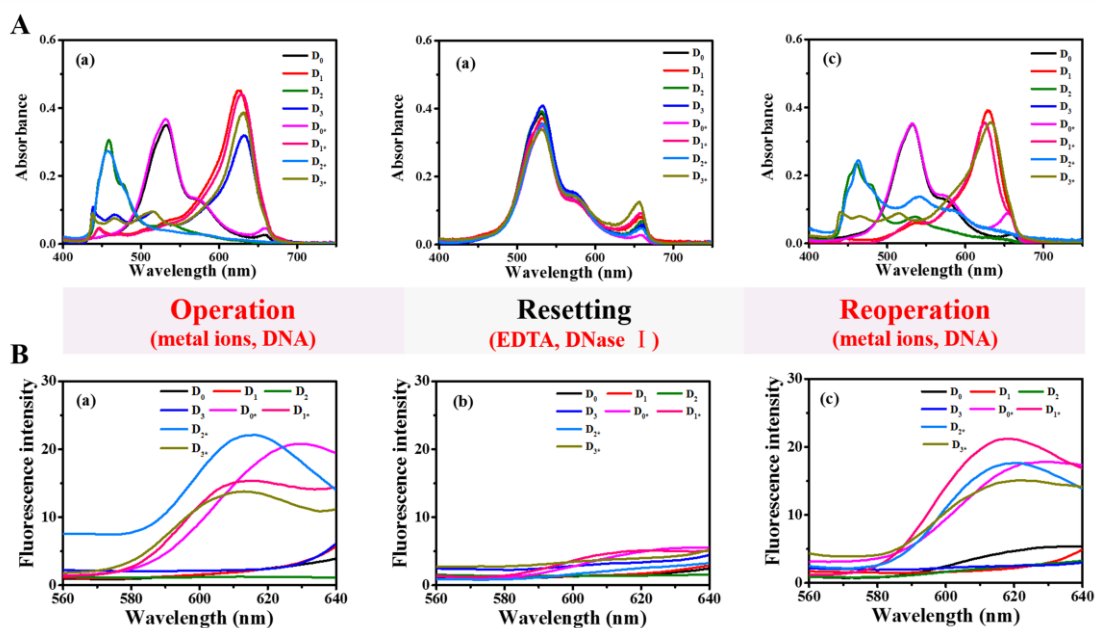


Fig. S19 (A) The absorption spectra of the 8-to-3 EC: operation (a), resetting (b) and reoperation (c). (B) The fluorescence spectra of the 8-to-3 EC: operation (a), resetting (b) and reoperation (c). The concentration of *MTC* is 6 μ M.

4. The spectra of the 14-to-4 EC

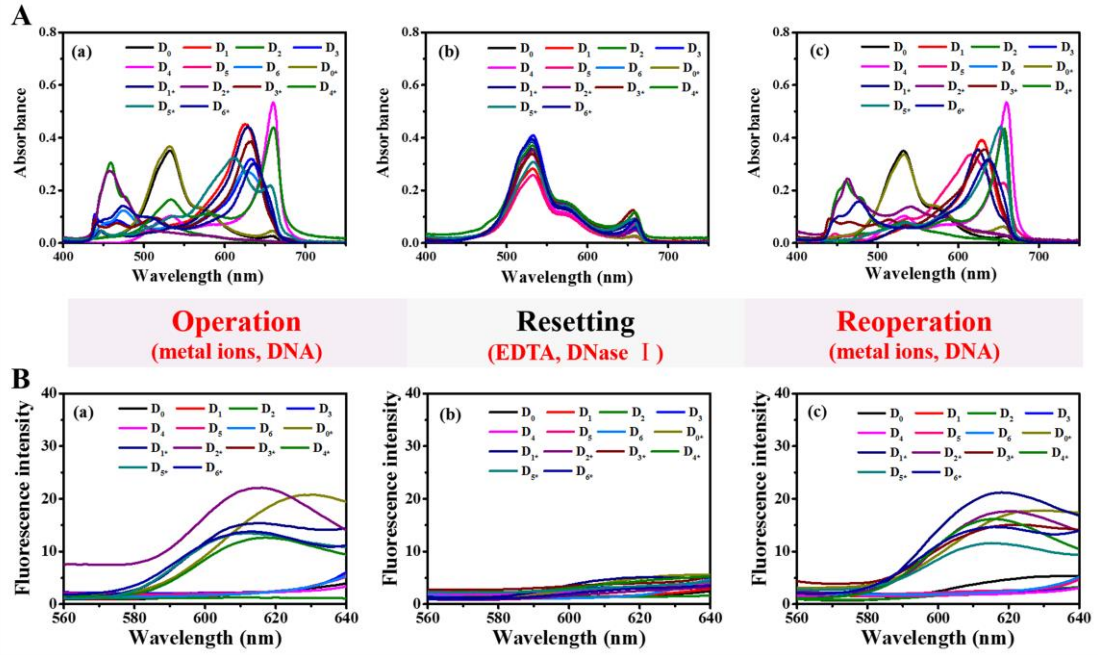


Fig. S20 (A) The absorption spectra of 14-to-4 EC: operation (a), resetting (b) and reoperation (c). (B) The fluorescence spectra of 14-to-4 EC: operation (a), resetting (b) and reoperation (c). The concentration of *MTC* is 6 μM .

5. The resetting and reoperation results in the 8-to-3 and 14-to-4 ECs

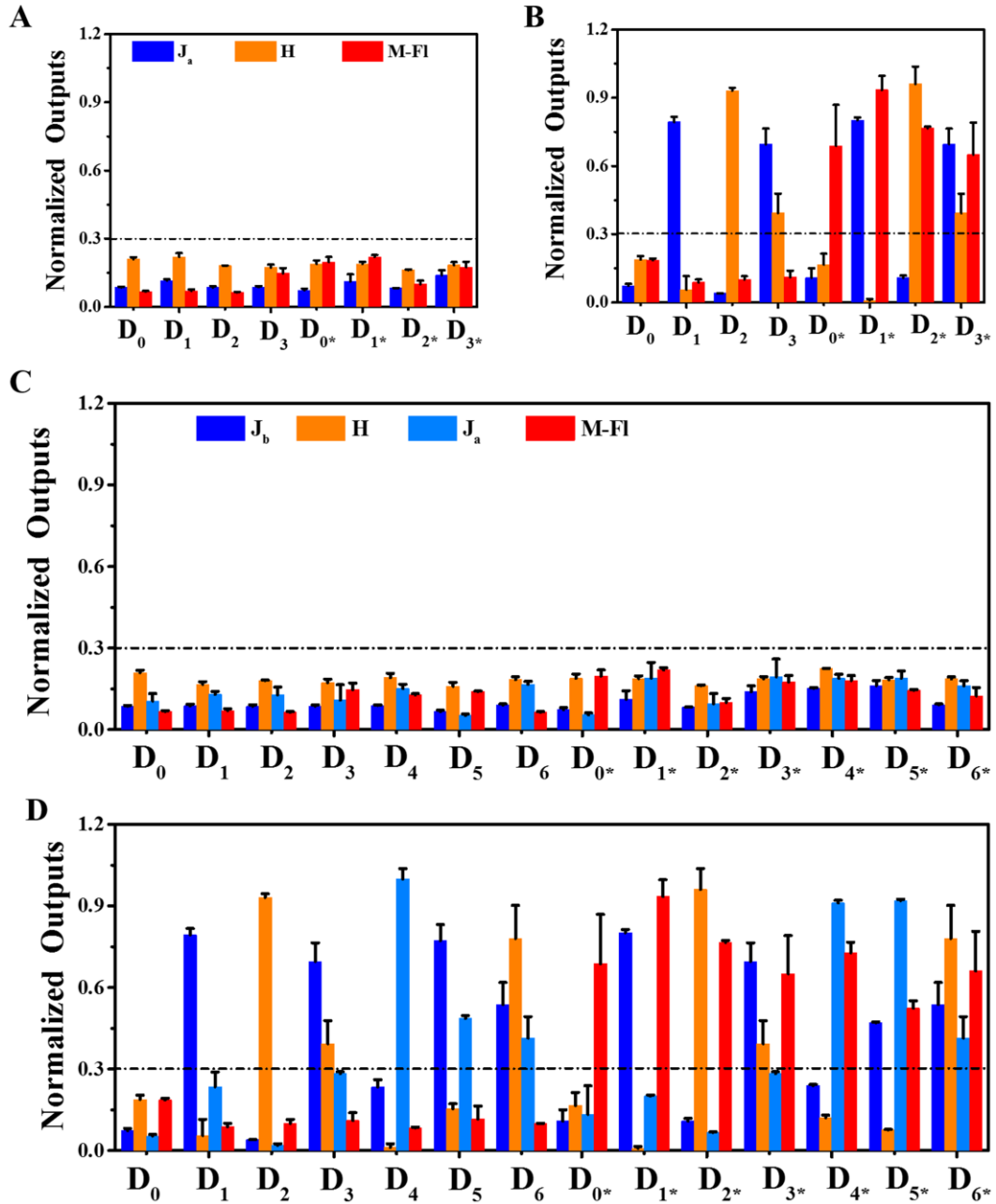


Fig. S21 The resetting (A) and reoperation (B) results of the 8-to-3 EC. The resetting (C) and reoperation (D) results of the 14-to-4 EC. The concentration of *MTC* is 6 μ M.

S(e) - The conversion between decimal and binary

A

				H	J_a	J_b	M-FI
0	Ag⁺	+	C₀	0	0	0	0
1	Ag⁺	+	G₀	0	0	0	1
2	Mg²⁺	+	C₁	0	0	1	0
3	Mg²⁺	+	G₁	0	0	1	1
4	Co²⁺	+	C₄	0	1	0	0
5	Co²⁺	+	G₄	0	1	0	1
6	Zn²⁺	+	C₅	0	1	1	0
7	Zn²⁺	+	G₅	0	1	1	1
8	Pb²⁺	+	C₂	1	0	0	0
9	Pb²⁺	+	G₂	1	0	0	1

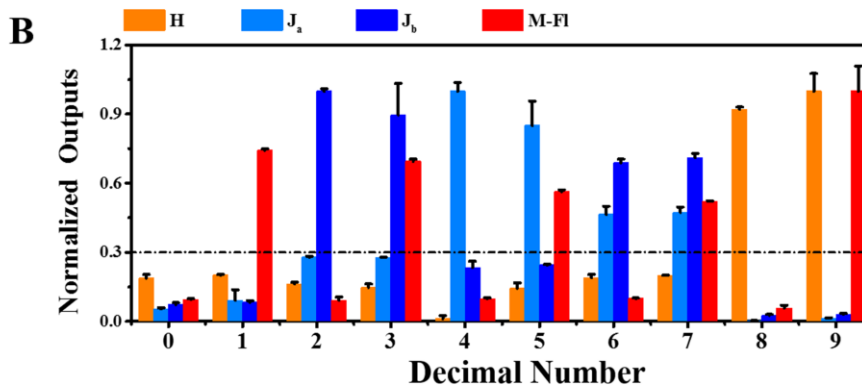


Fig. S22 (A) The schematic truth table of the conversion between decimal and binary. (B) The normalized outputs of the conversion.

S(f) - The temperature effect on the ECs

1. The temperature effect on the *MTC* aggregations and the *MTC*-DNA complex

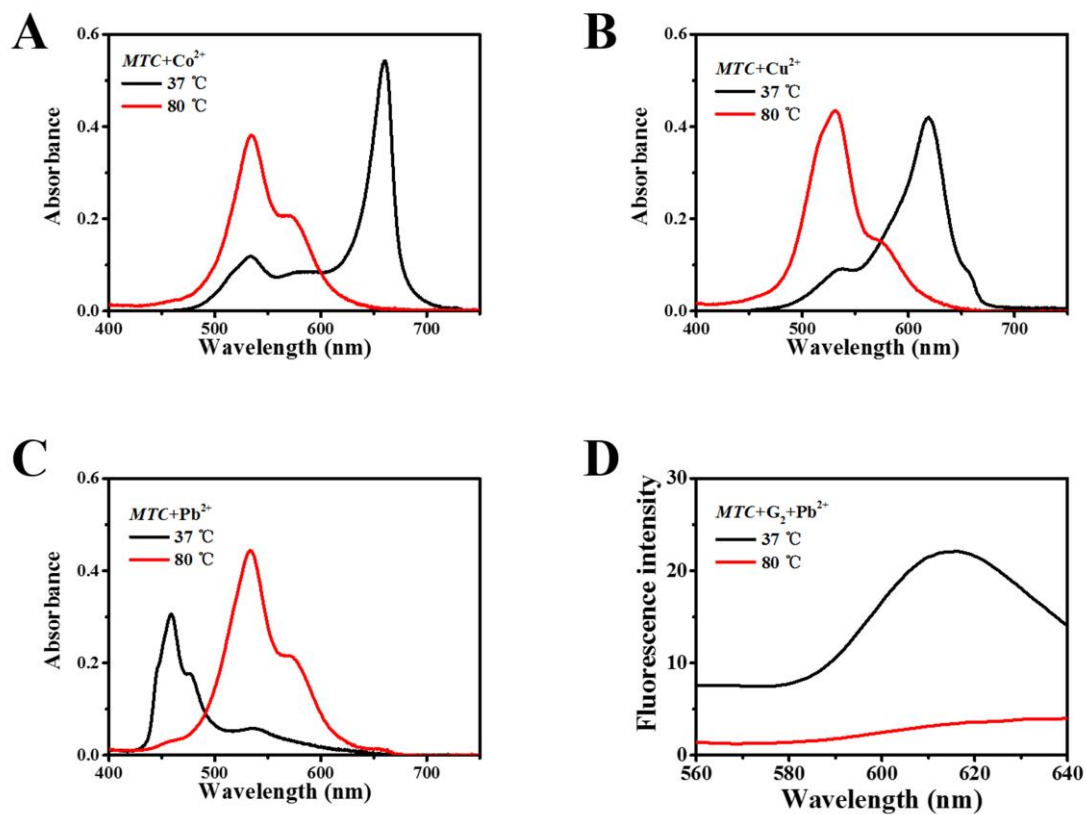


Fig. S23 The temperature effect on the *MTC* J_a-aggregates (A), J_b-aggregates (B), H-aggregates (C) and the *MTC*-DNA complex (D). The concentration of *MTC* is 6 μ M.

2. The 8-to-3 encoding function was shut down by a high temperature

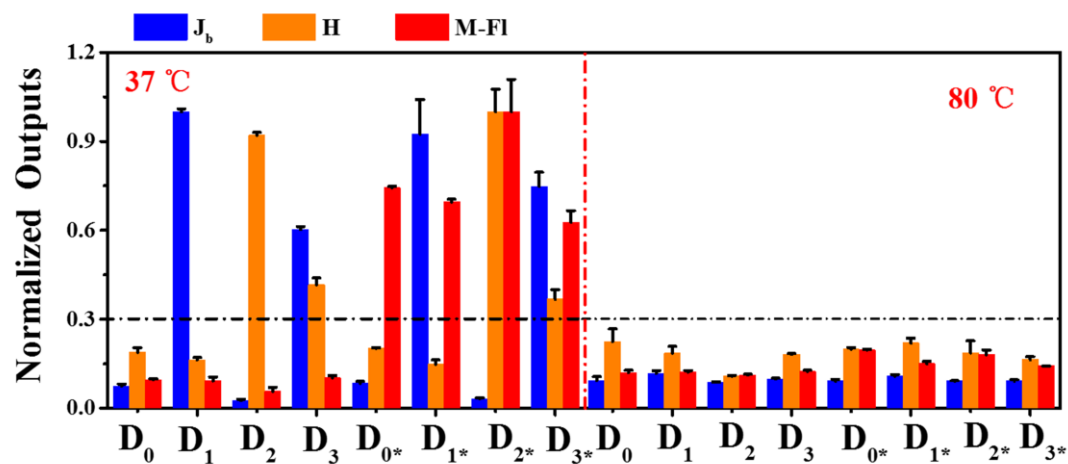


Fig. S24 The normalized outputs of the 8-to-3 EC in 37 °C and 80 °C respectively. The concentration of *MTC* is 6 μ M.

References

1. F. M. Hamer, *The cyanine dyes and related compounds*, Interscience Publishers, New York,, 1964.
2. G. E. Ficken, *The Chemistry of Synthetic Dyes*, Academic Press, New York, 1971.
3. H. A. Assi, R. El-Khoury, C. Gonzalez and M. J. Damha, *Nucleic Acids Res.*, 2017, 45, 11535-11546.
4. T. Li, E. K. Wang and S. J. Dong, *J. Am. Chem. Soc.*, 2009, 131, 15082–15083.
5. X. H. Zhou, D. M. Kong and H. X. Shen, *Anal. Chem.*, 2010, 82, 789-793.
6. Q. Yang, J. Xiang, S. Yang, Q. Li, Q. Zhou, A. Guan, X. Zhang, H. Zhang, Y. Tang and G. Xu, *Nucleic Acids Res.*, 2010, 38, 1022-1033.
7. S. Xu, Q. Li, J. Xiang, Q. Yang, H. Sun, A. Guan, L. Wang, Y. Liu, L. Yu, Y. Shi, H. Chen and Y. Tang, *Nucleic Acids Res.*, 2015, 43, 9575-9586.